systems

MDPI

Article

Risk Simulation of Urban Rainstorm Flood Disasters Considering Crowd Activities

Jing Huang [1], Tiantian Pang [1], Zhenzhen Liu [1], Zhiqiang Wang [2] and Huimin Wang [1,*]

[1] Management Science Institution, Hohai University, Nanjing 211100, China; j_huang@hhu.edu.cn (J.H.); tianpang@hhu.edu.cn (T.P.); liuzhenzhencs@hhu.edu.cn (Z.L.); zhiqiang.wang@zufe.edu.cn (Z.W.)
[2] College of Information Management and Artificial Intelligence, Zhejiang University of Finance and Economics, Hangzhou 310018, China
* Correspondence: hmwang@hhu.edu.cn; Tel.: +86-13951674321

Abstract: Social activities have a significant impact on the rainstorm flood disaster risk. It is crucial to explore the dynamic changes of urban rainstorm flood disaster risk caused by crowd activities. In this study, a risk simulation method of urban rainstorm flood disasters is proposed, composed of an urban rainstorm flood model based on SWMM and LISFLOOD-FP and a crowd activities model based on ABM. Taking the Futian District of Shenzhen as an example, the temporal and spatial changes in rainstorm flood disaster risk for buildings and roads are analyzed under three scenarios: midnight, morning peak, and evening peak. The results show that: (1) Although the overall risk of urban rainstorm flood disasters increases as the inundation area expands, the average risks of roads and buildings increase rapidly and then stabilize during the morning peak due to commuting activities, while the average risk of roads remains high level during the evening peak due to commuting activities, while; (2) The risk of urban rainstorm flood varies significantly at different time periods. The average risk of buildings is the largest during the morning peak, about twice that during the evening peak. The number of high-risk roads during the evening peak is much higher than in the morning peak, and both buildings and roads have the least risk during midnight; (3) The spatial distribution of urban rainstorm flood disaster risk changes with the crowd activities, shifting from residential areas to industrial areas, schools, shopping malls, etc., during the morning peak, while the evening peak shows the reverse.

Keywords: urban rainstorm flood; risk simulation; crowd activities; agent-based model

Citation: Huang, J.; Pang, T.; Liu, Z.; Wang, Z.; Wang, H. Risk Simulation of Urban Rainstorm Flood Disasters Considering Crowd Activities. *Systems* **2023**, *11*, 407. https://doi.org/10.3390/systems11080407

Academic Editor: Ed Pohl

Received: 27 April 2023
Revised: 4 August 2023
Accepted: 6 August 2023
Published: 8 August 2023

1. Introduction

Rainstorm flood disasters have become a prominent problem affecting urban public safety. Exploring the temporal and spatial variation law of exceptionally heavy rainstorm flood disaster risk is of great significance for emergency response plans for rainstorm flood disasters, which contributes to optimizing and improving the emergency handling capacity of urban rainstorm flood disasters and ensuring urban public safety. With the acceleration of urbanization, the urban water cycle processes have undergone drastic changes, and the "heat island effect" and "rain island effect" are prominent, resulting in more and more frequent urban rainstorm flood disasters. At the same time, a large number of people have poured into the city, and the lives and work of humans have undergone tremendous changes. Due to activities such as life, work, and entertainment, the frequency, intensity, and scale of people shuttling between work and their homes, neighborhood parks, crowded markets, and busy streets is increasing. The frequent spatial movement of the population increases the exposure of the disaster-bearing body, further enhances the risk of rainstorm and flood disasters, and aggravates the threat degree of urban rainstorms and flood disasters to human society. Taking the "July 20" heavy rainstorm in Zhengzhou in 2021 as an example, the central urban area of Zhengzhou suffered a serious urban rainstorm

flood disaster in a short period of time, which seriously affected people's work, shopping and commuting, especially the serious irrigation incident of Metro Line 5, resulting in 14 deaths and heavy losses [1]. The huge population size and complex crowd activities in cities have further posed enormous challenges to the emergency management of urban rainstorm flood disasters.

In the field of urban rainstorm flood disaster risk research, scholars have mainly focused on two aspects: probability-based studies and impact-consequence studies [2–4]. The former defines risk as the probability of disasters occurring due to the interaction of natural or man-made hazards with vulnerability conditions [5]. The latter assesses the risk of disasters by analyzing potential hazards and evaluating existing exposure and vulnerability conditions [6,7]. The Hazard–Exposure–Vulnerability framework is widely used to assess urban rainstorm flood risk [8–10], which is comprehensive, clear and has great operability. At the same time, flood risk studies have changed from static risk maps to dynamic risk simulations. There are a large number of studies based on hydrological and hydrodynamic models to simulate flood processes under different rainstorm recurrence periods [11,12]. Studies on flood risk management and assessment are carried out by drawing flood risk maps of submerged water depth and inundation range [13–16]. Where only the dynamic evolution of the urban flood process has been considered, there is a lack of research on the vulnerability of the rainstorm environment and the dynamic exposure of the bearer.

However, flood disasters are complex systems formed by the interaction of natural disaster systems and human social systems [17,18]. Rainstorm flood disaster risk is shaped by the inundation process formed by heavy rainfall runoff and the interaction of social crowd activities. Studies have suggested that the complex spatial activities of urban crowds will further enhance the risk of rainstorm flood disasters and aggravate the losses of urban rainstorm flood disasters [19,20]. With the advancement of technology and the availability of spatiotemporal geographic big data, scholars have begun simulating urban crowd activities using Agent-Based Model (ABM) [21–23] and tried to study the risk of rainstorm flood disasters. For example, Lai et al. [24] constructed an agent-based risk assessment system according to the dynamic and complex characteristics of rainstorm flood house exposure, which verified the feasibility of introducing the Agent-Based Model theory for the dynamic assessment of rainstorm flood disaster risk; Dawson et al. [25] and Li et al. [26] coupled crowd dynamic activities, constructed a population risk assessment model of rainstorm flood based on ABM; Dai et al. [27] proposed a human–disaster coupled urban model (HazardCM) to analyze the exposure of population in flood disaster environment. Although the above scholars have tried to incorporate crowd activities into flood risk systems to study the vulnerability and exposure characteristics of rainstorm flood disasters, flood disaster risk studies under different crowd activity scenarios are still relatively lacking and need to be further explored.

This study aims to explore the impact of complex urban crowd activities on urban flood risk. Using a "bottom-up" modeling approach, an urban rainstorm flood disaster risk simulation model is constructed, which includes an urban rainstorm flood model based on SWMM and LISFLOOD-FP and a crowd activities model based on ABM. The study explores the dynamics risk of buildings and roads under different flooding scenarios is explored in the Futian District of Shenzhen City, China, to provide effective support for disaster prevention and mitigation management of urban rainstorm flood disasters.

2. Methods and Data

2.1. Risk Formation and Assessment of Urban Rainstorm Flood Disasters Considering Crowd Activity

The occurrence of a rainstorm flood event is a natural phenomenon, and the concept of risk does not solely depend on where the storm flooding takes place. Rather, it is when the disaster causes certain damages to human society or places of human social activities that the risk of a rainstorm flood disaster exists. In urban areas, when rainstorm flood disasters

occur, the social population and natural disasters interact in both time and space, forming a complex system of urban rainstorm flood disaster risk [28]. Therefore, a systematic analysis of the formation mechanism of disaster risk is crucial to accurately simulate the risk process of urban rainstorm flood disasters.

According to the system theory, the rainstorm flood disaster risk system consists of three parts: disaster-causing factors, disaster-inducing environment and disaster-bearing body:

(1) The disaster-causing factors refer to the elements that have adverse effects on people's life, property or various activities and may lead to disasters. For rainstorm flood disasters, these factors mainly include the intensity of the rainstorm and the depth of flooding. Usually, the greater the intensity and inundation depth, the more severe the damage and loss, resulting in higher risk. The degree of influence of disaster-causing factors is expressed by the hazard degree.

(2) The disaster-inducing environment pertains to the spatial and geographical surroundings where the rainstorm occurs, particularly buildings and roads in urban areas. Environmental sensitivity refers to the extent of response (sensitivity) to the external environment in the area when exposed to disaster-causing factors. If the sensitivity of buildings or roads in the affected area is higher at the same intensity of disaster-causing factors, the resulting damage and risk of the disaster will be more severe. The degree of flood risk influenced by the environment is expressed as sensitivity.

(3) The disaster-bearing body refers to the entities that are susceptible to various disaster-causing factors, typically including the concentration and distribution of population and various resources within a specific area. Generally, higher concentrations of population and property in an area correspond to a higher risk of disasters. Exposure quantifies the level of risk that the disaster-bearing body faces in relation to the potential of flooding or other disaster events. It reflects the degree to which the disaster-bearing body is vulnerable to the impact of such events.

Therefore, the complex spatial and temporal dynamics of urban rainstorm flood disaster risk depend on the rainstorm flood event, crowd activities, and urban spatial environment. Based on the "H-E-V" framework, as shown in Figure 1.

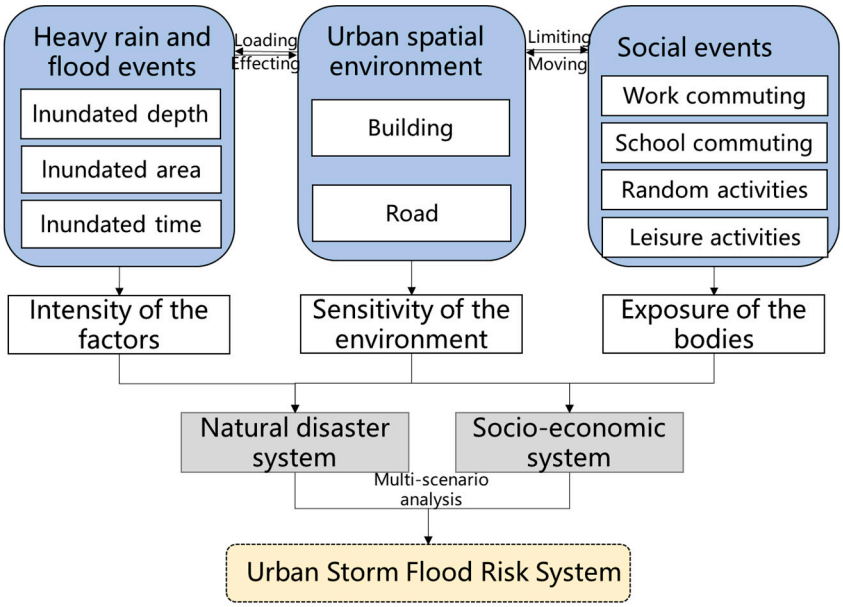

Figure 1. Urban rainstorm flood disaster risk formation mechanism.

Considering the interaction among disaster-causing factors, disaster-bearing bodies and disaster-inducing environment, urban rainstorm flood disaster risk is defined as the degree of damage that may be caused to the city or the degree of impact on human society

after a rainstorm flood disaster occurs. The risk is considered to consist of hazard, exposure and vulnerability:

That is, urban rainstorm flood risk = Hazard (H) × Exposure (E) × Vulnerability (V).

Hazard refers to the intensity and inundation depth of the flood disaster process, which is used to characterize the dynamic changes in the hazard level of the causal factors during the flooding event. Exposure refers to the degree of exposure to the risk factors affected by flood disasters [29], and this study refers specifically to the urban population exposed to urban rainstorm flood disasters, and the most characteristic of the exposure of the population carrier is the spatial distribution of the population density at different moments. Given that the population is still in a dynamic state of activity during the occurrence of disasters, the precise location and simulation of the spatial and temporal distribution of the population is a key element in assessing the spatial and temporal distribution of the risk of the rainstorm flood. Vulnerability, here, specifically sensitivity, refers to the ability of the urban geographic environment to resist the adverse effects of storm flooding [30]. In this study, it refers to the sensitivity of two types of geographic entities, buildings and roads, to heavy rainstorm flood disasters in the city.

Therefore, the mathematical formula for risk calculation in the simulation model of urban rainstorm flood disaster risk for roads and buildings constructed in this study is:

$$R_i = H_i \times S_i \times (P_i / A_i) \quad (1)$$

$$R_j = H_j \times S_j \times (P_j / A_j) \quad (2)$$

where R_i denotes the risk of the road i; R_j denotes the risk of building j; H_i denotes the depth of inundation of the road i; H_j denotes the depth of inundation of the building j; S_i denotes the sensitivity of the road i to heavy rainstorm flood disasters; S_j denotes the sensitivity of the building j to rainstorm flood disasters; P_i denotes the total number of people located on the road i; P_j denotes the total number of people located in the building j; A_i denotes the total area of the road i; and A_j denotes the total area of the building j.

2.2. Risk Simulation Modeling of Urban Rainstorm Flood Disasters Based on ABM

2.2.1. Framework of Risk Simulation Modeling

The urban rainstorm flood disaster risk exhibits distinct spatiotemporal dynamics, which are not only influenced by the evolution of flood hazards but also by the dynamic movement of the urban population, intricate relationships, and non-linear interactions between disasters and the environment. To comprehensively capture the process from micro-individual dynamic changes to the macro-emergence of risk for each element of urban rainstorm flood disasters, this study integrates the process of rainstorm flood and the process of crowd activities based on the modeling method of ABM. The model superimposes the flooding process on the physical spatial environment of urban buildings and roads and then constructs three rainstorm flood disaster scenarios of morning peak, evening peak and midnight. It updates the urban flood map in real time to dynamically display the whole process of the dynamic evolution of rainstorm flood disasters in real time. The framework of the urban rainstorm flood risk simulation model is constructed as shown in Figure 2.

The inundation depth of the road and the buildings are simulated based on urban rainstorm flood modelling in Section 2.2.2. The crowd activities are simulated based on environment construction and agent-based modelling in Sections 2.2.3 and 2.2.4, respectively. The urban rainstorm flood disaster risk for roads and buildings is calculated using Formulas (1) and (2). Three scenarios are constructed in this study: morning peak, evening peak, and midnight. Morning peak is set during 6:00 a.m.–10:10 a.m., the period of high population activity in the morning, typically around the rush hour when people are commuting to work or school. The evening peak is set from 17:00 p.m.–21:10 p.m., another peak time of the day for the population when people return home after a day of work and

study. The midnight scenario refers to the period between 0:00 a.m. and 4:10 a.m. when the city's population is almost stationary.

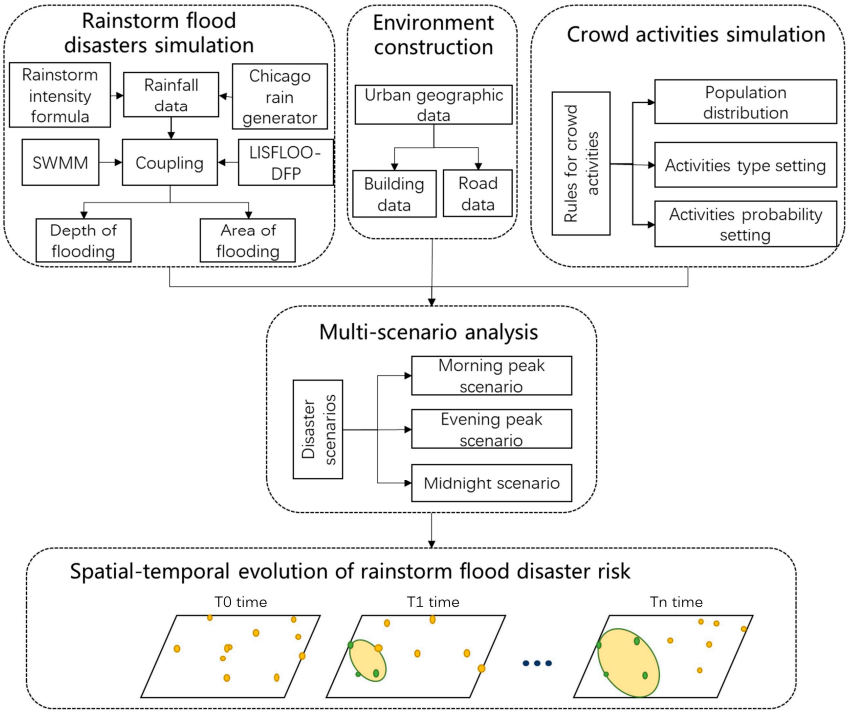

Figure 2. Urban rainstorm and flood disaster risk simulation framework.

2.2.2. Urban Rainstorm Flood Modelling

In this study, the generalization of the study area was carried out using the ArcGIS platform, which involved generalizing pipe network data, delineating sub-catchments, and determining outlets. SWMM (Storm Water Management Model) and LISFLOOD-FP models are coupled to simulate urban surface hydrological processes and underground pipe network hydrodynamic processes, thereby enabling the simulation of the inundation range and depth during rainstorms and flood [27,31].

The SWMM model is a distributed hydrological and hydrodynamic model that is composed of three main parts: hydrology, hydrodynamics, and water quality. It can comprehensively simulate the variation of water quantity and quality in urban drainage systems. It is used to simulate the rainfall, surface production flow, pipe network confluence and pipe network overflow process. The drainage system is generalized into a series of pipe sections and pipe network nodes (such as stormwater grates and inspection wells), where the runoff transmission in the drainage pipe network obeys the conservation of mass and momentum; The flow velocity and water depth in the pipeline are solved by the Sanint–Venant equation system of the hydrodynamic method, that is, the continuous equation and the momentum equation are solved simultaneously to simulate the gradual non-constant flow and realize the pipe network convergence simulation.

The LISFLOOD-FP model is a two-dimensional hydrodynamic model based on a square grid developed by the University of Bristol. It simulates one-dimensional river hydraulic changes and two-dimensional floodplain hydraulic changes through continuity equations and momentum equations. As a semi-open source model that is easy to build and has high computational efficiency, the LISFLOOD-FP model has been widely used in the two-dimensional simulation study of urban waterlogging and river flooding [32]. The LISFLOOD-FP model is used to simulate the inundation process of nodal overflow and rainfall runoff on the urban surface. Based on the DEM of the study area, the continuity equation and the momentum equation are used to consider the water balance between adjacent grids.

The SWMM model is proficient in simulating confluence in underground drainage pipe networks, but it cannot simulate the surface confluence process to obtain the inundation range, water depth and the flood process of the urban surface. Meanwhile, the LISFLOOD-FP model can simulate the surface runoff process, but it cannot simulate the water flow of the underground pipe network. Coupled SWMM with LISFLOOD-FP can obtain the water exchange between the surface flow runoff and the underground drainage pipe network to simulate the urban surface hydrological process and the underground pipe network hydrodynamic process. The exchange of water volume between the drainage pipe network and the surface can be generalized as rainfall collects on the surface production flow to form runoff from the pipe network node into the drainage pipe network and when the drainage capacity of the drainage pipe network is insufficient, the amount of water overflows through the pipe network node and flows into the surface runoff; When the drainage network regains drainage capacity, surface runoff rejoins the drainage network.

2.2.3. Environment Construction

As a natural space susceptible to torrential rainstorm flood disasters, the geographical environment not only provides a living space for agents in the simulation model but also links flood disasters with crowd activities. Two types of disaster simulation environments for buildings and roads are constructed:

a. Buildings serve as spaces for population activities and survival, providing temporal and spatial constraint attributes for the urban population and rainstorm disasters. These attributes include the area, type, sensitivity to rainstorm flood disasters, number of people, inundation depth of the flood, and corresponding types of crowd activities. According to the type of travel activities of urban people and land use classifications [33,34], building types are divided into six categories: parks, residential areas, industrial areas, shopping malls, schools, and others. According to the previous studies [35], the sensitivity to rainstorms of each building type is set as follows: schools are classified as level 1 sensitivity, shopping malls and industrial areas as level 2 sensitivity, residential areas as level 3 sensitivity, and parks and others as level 4 sensitivity.

b. Roads are another important aspect of crowd dynamic activities. The properties of roads include the length, width, type, and sensitivity of heavy rainstorm flood disasters, the number of residents, and the inundation depth of the flood. Roads are divided into four categories: main roads, secondary roads, motorcycle roads and community branch roads. According to the road design standards and traffic volume in the "Urban Road Design Code"(CJJ37-2012), the sensitivity to rainstorms of each road type is set as follows: community branch road as level 1 sensitive, highway as level 2 sensitive, secondary road as level 3 sensitive, main road as level 4 sensitive. Finally, the sensitivity is assigned values ranging from 0.1 to 1 using the natural discontinuity method.

2.2.4. Crowd Activities Modelling Based on ABM

Agent-Based Modeling (ABM) aims to simplify complex adaptive systems into individual agents and simulate the entire system from the bottom up, thereby capturing complex changes in the global system through the interactions and behavior of local agents with each other and the environment. ABM offers distinct advantages in simulating and analyzing the evolution of complex adaptive systems. Urban rainstorm flood disaster risk is a typical complex system, and the ABM-based modelling method is well-suited to depict the process from micro-level dynamic changes of urban rainstorm flood disaster elements to macro-level risk emergence. This approach provides a novel research idea for studying urban rainstorm flood disaster risk. In light of this, the current study employs ABM to simulate the spatiotemporal changes in rainstorm flood disaster risk influenced by time factors.

The urban population, being the main affected group during urban rainstorm flood disasters, engages in complex spatial and temporal activities that significantly impact the change in urban rainstorm flood risk. The construction of an Agent-Based Model can

change its spatiotemporal coordinates based on different time drivers and more accurately describe the complex individual heterogeneous activities of the population [36]. Using the existing data of the urban census, the urban population is categorized into four categories according to the different travel behaviors of the population: student population, working population, random population and elderly population, as shown in Table 1. Subsequently, the daily travel activities of the urban population are classified into types, such as going home, working, studying, shopping, and leisure, based on travel behavior surveys and analyses.

Table 1. Description of urban population classification.

Type	Properties
Student population	Students aged 3–14 engaged in activities such as going to school, going home and leisure
Working population	Aged 20–59 with regular jobs, part of the employed population has children and participates in activities such as going to work, going home, picking up children, shopping, leisure, etc.
Random population	Individuals without regular jobs, involved in leisure activities, some have children
Elderly population	Seniors over 59 years old participating in activities such as transporting children, going home, leisure, and shopping

After the classification, four different types of population agents are constructed based on the different types of crowd activities [37]. The agents' behavior rules are established using a probabilistic deduction model [38]. The spatiotemporal coordinates of these agents are modified based on various time drivers, linking the population with the spatial environment and enabling the simulation of the daily commuting activities of the urban population. The activity rules for each of the four types of population agents are shown in Figure 3.

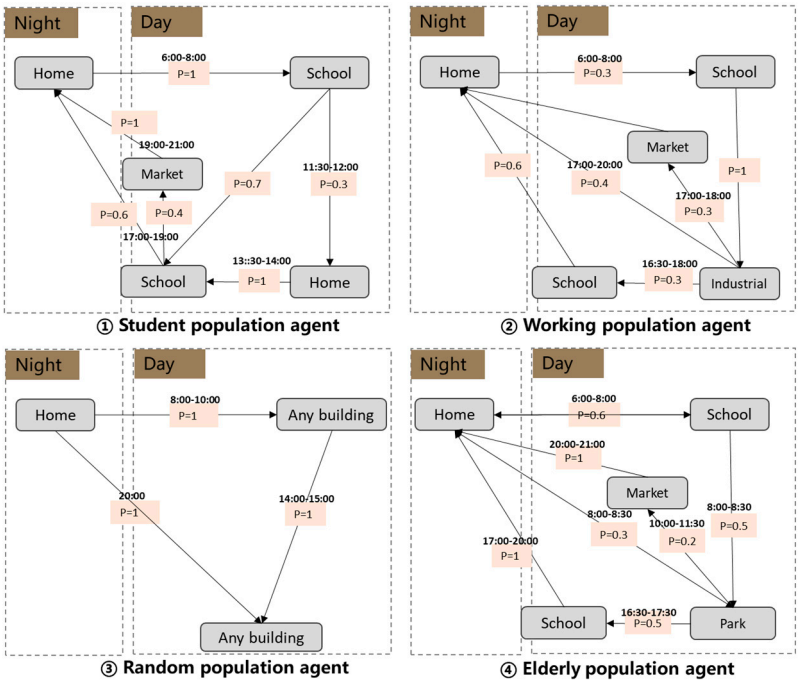

Figure 3. Rules for four types of population agents.

a. Student population: They leave their residences for school at around 7:00 a.m. and stay at school until around 11:30 a.m., with a 30% chance of returning home for lunch. After that, they return to school around 1:00 p.m. to continue studying. After 5:00 p.m. in the

afternoon, they either return home from school or go to the nearby shopping malls or parks for leisure, and at 9:00 p.m., they end the day's activities and return to their residences.

b. Working population: Around 30% of the working population sends their children to primary school at 7:00 a.m. and then goes to the industrial areas to work. They stay in the workplace until about 4:30 p.m., with a 30% chance of going to school to pick up their children before returning home. After 5:00 p.m., there is a 40% probability of going home directly and a 30% probability of going to the shopping malls. At 9:00 p.m., the day's activities end, and all return to their residences.

c. Random population: This group includes individuals in a random state in the population system, such as taxi drivers and tourists, who move randomly within the city space. They start random activities away from home at 8:00 a.m., end all activities at 8:00 p.m., and return to their residences to rest.

d. Elderly population: Around 7:00 a.m. in the morning, 60% of the elderly begin by sending their children to school and then engage in leisure, entertainment, dining, or shopping activities. They pick up their children from school in the evening and then return home after a day's activities. On the other hand, 40% of the elderly go to parks, shopping malls or other leisure and entertainment places, or some stay at home; they return home at 11:30 a.m. to rest and then continue leisure or dining and shopping activities at 2:00 p.m. with a 50% probability All activities end at 9:00 p.m., and they return to their residences to rest.

2.3. Study Area and Data

2.3.1. Study Area

Futian District, as shown in Figure 4, is located in the central urban area of Shenzhen. It serves as the administrative, financial, cultural, commercial, and international exchange center of the city. The district falls under a subtropical maritime monsoon climate with long summers and short winters, abundant sunshine, and significant rainfall. The average annual rainfall in the past five years (2018 to 2022) is 1926.8 mm. As a result, the area is susceptible to extreme weather events such as rainstorms, local heavy rainstorms, or exceptionally heavy rainstorms.

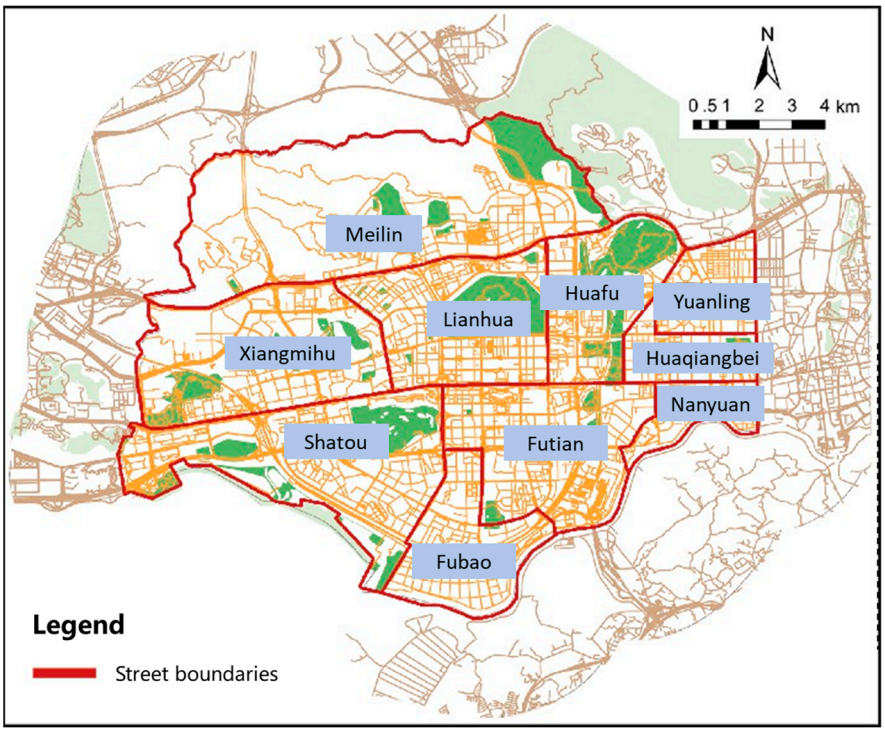

Figure 4. Location of Futian District, Shenzhen.

Futian District is composed of 10 streets, including Yuanling Street, Nanyuan Street, Futian Street, Shatou Street, Meilin Street, Huafu Street, Xiangmihu Street, Lianhua Street, Huaqiang North Street, and Fubao Street, with a total of 95 communities and 115 neighborhood committees. According to the Shenzhen Statistical Yearbook, its permanent population is about 1,553,200 in 2021, including 247,500 individuals aged 0–14, accounting for 15.94% of the total population. The population aged 15–59 is 1,174,700, accounting for 75.63%, while the population aged 60 and above is 131,000, accounting for 8.43%, with approximately 85,000 individuals, or 5.47%, being aged 65 and above.

2.3.2. Data Collection

The research data mainly include basic geographic data, population data and rainstorm flood inundation data, as detailed in Table 2. Road network data is downloaded from the OpenStreetMap website. Buildings, drainage pipe networks, and waterlogging points monitoring data are obtained from Shenzhen Hydrology Bureau. The population data is collected from China's statistical database. The inundation data is collected from the Meteorological Bureau of Shenzhen Municipality. Waterlogging points monitoring data.

Table 2. Collection of the study data.

Name	Description	Source
Road network	Vector geographic data, including road type, road length, road name and other attributes	OpenStreetMap website (www.openstreetmap.org (25 July 2023))
Building	Vector geographic data, including building type (such as hospitals, schools, industrial areas, residential areas, etc.), building area	Shenzhen Hydrology Bureau
Drainage network	Vector geographic data, including inspection wells, water outlets, rainwater lines, drainage lines	Shenzhen Hydrology Bureau
Population data	Statistical data of total population for each subdistrict, sex ratio, proportion of elderly people and children.	China statistical database (http://www.shujuku.org/shenzhen-statistical-yearbook.html (25 July 2023))
Rainstorm flood inundation	Inundation data on 29 August 2018, and 11 April 2019, in Shenzhen	Shenzhen Meteorological Bureau (http://weather.sz.gov.cn/qixiangfuwu/qihoufuwu/qihouguanceyupinggu/jiancegongbao/index_2.html (25 July 2023))
Waterlogging points monitoring data	Monitoring data of Waterlogging points on 29 August 2018, and 11 April 2019, in Shenzhen	Shenzhen Hydrology Bureau

2.3.3. Model Initialization

GAMA (https://gama-platform.org/wiki/Home (25 July 2023)) is an open-source modeling and simulation environment for creating spatially explicit agent-based simulations. It can also load geospatial data very well. GAMA can effectively combine time and space to simulate urban crowd activities in the real world. In addition, GAML language has the characteristics of a fully programmable, simple language structure, can define unlimited agents and variables, support cross-platform, reusable, etc. So, it is especially suitable for the modeling of urban rainstorms and flood disaster risk complex systems, which involve multiple subject types.

In the study, the data for the study area was initialized using the GAMA platform. This initialization process involved the following steps: Firstly, the vector geographic data was initialized in the study area; there were 3106 buildings categorized into different

zones, such as residential, industrial, school, shopping mall, and park buildings. The total construction area was 386,000 square kilometers, with a total of 4598 road sections and a cumulative mileage of 94,500 km. Secondly, according to the "The Seventh National Census Bulletin of Shenzhen City" (http://tjj.sz.gov.cn/ztzl/zt/szsdqcqgrkpc/szrp/index.html (25 July 2023)), the ratio of population agents of each type was set according to the gender and age ratio data of the population of each street. The number of all kinds of agents in the model was generated in a ratio of 1:30 and allocated to each residential building according to the building area. Finally, the model start time was set at 0:00.

Table 3 provides a summary of the specific initialization parameters used in the simulation model. These parameters were essential for creating a realistic and dynamic simulation of urban rainstorm and flood disaster risks, considering the spatiotemporal dynamics of crowd activities and their interactions with flood hazards in the study area.

Table 3. Simulation model initialization parameters.

Variables	Unit	Meaning	Initial Value
start_date	Date	Assumed time for model initialization	1 July 2025
step	Step length	The model runs one loop corresponding to a realistic time	10
current_hour	Hours	Current Time	0
current_min	Minutes	Current Time	0
nb_workingpeople		Number of initialized workforce	30,420
nb_childrenpeople		Number of the initialized student population	8298
nb_oldpeople		Number of elderly populations initialized	4667
nb_randompeople		Number of random populations initialized	8475
flood_depth	meters	The current moment of torrential rain flooding	0
min_work_start		Earliest start time of the working population	7
max_work_start		The latest start time of the working population	8
min_work_end		Earliest closing time of the working population	17
max_work_end		The latest start time of the working population	20
min_speed	km/h	Minimum movement speed of population intelligence	5
max_speed	km/h	Maximum movement speed of population intelligence	15

Based on vector geographic building data, this study conducted secondary modeling and distribution of population distribution, realized population density mapping at the building scale, and realized spatialization of urban population data. To estimate the population contained in each individual urban residential building, a mathematical model was established using the building space area attribute and population density grid [39]. The calculation formula for estimating the population in building i is as follows:

$$POP_i = \alpha * S_i + e \tag{3}$$

POP_i is the estimated population contained in building i; S_i is the total area of building i; α is the scale coefficient value, which is 0.021; e is the error.

The population in the grid was allocated to each residential building according to the area proportion of buildings. Next, the inundation simulation results of the once-in-a-century rainfall in the Futian District of Shenzhen City were superimposed with the basic geographic information data of the district. This process involved converting the rainstorm inundation data into the inundation attribute of buildings and roads.

And finally, the initialization interface of the simulation model was obtained, as shown in Figure 5. This interface serves as the starting point for the simulation model, incorporating the spatiotemporal dynamics of rainstorm flood disasters and crowd activities in the study area, allowing for a comprehensive understanding of the urban rainstorm flood disaster risk.

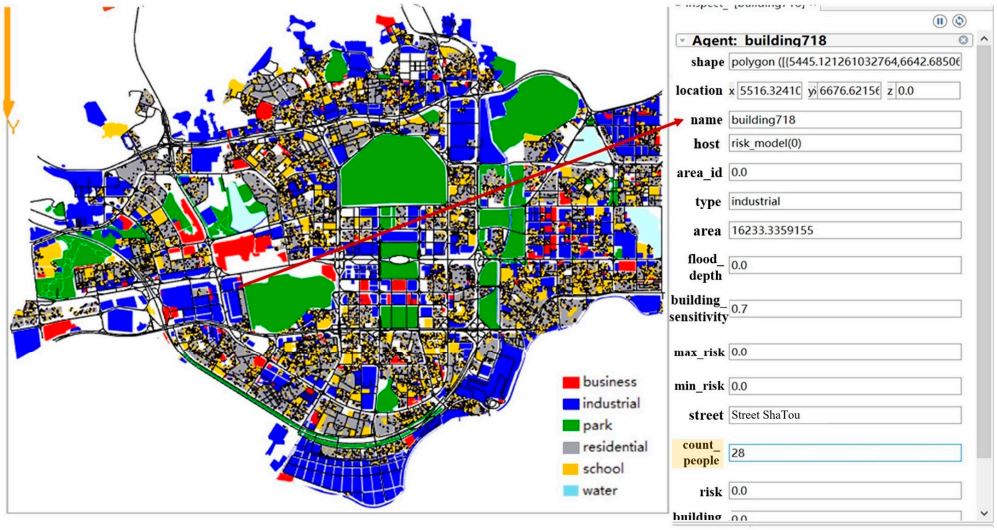

Figure 5. Basic geographic data and population initialization of Futian District, Shenzhen.

3. Results of Rainstorm Flood Disaster Risk

3.1. Result of Urban Rainstorm Flood Disaster Simulation

Using the Chicago rain pattern, the rainfall process of once-in-a-century in the study area was calculated. Subsequently, the SWMM-LISFLOOD-FP coupling model was used to simulate the flooding process of this once-in-a-century rainstorm in the Futian District. To determine the optimal parameters for the coupling model, the method of multiple selection and calculation of multiple values of the two rainstorm flood data on 29 August 2018, and 11 April 2019, was used. The results of the simulation indicate that the largest inundation of precipitation in the Futian District during the once-in-a-century event is illustrated in Figure 6.

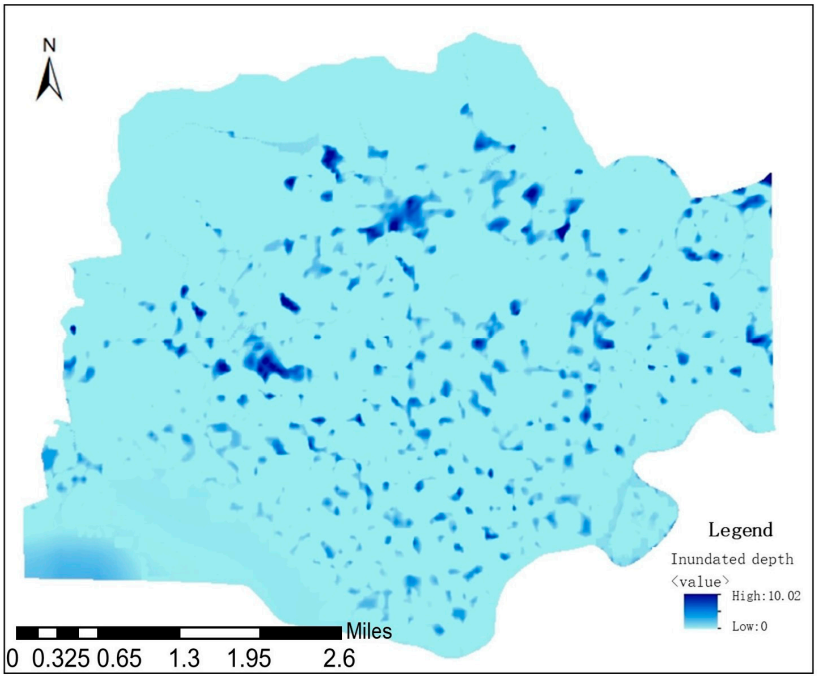

Figure 6. The largest inundation in Futian District.

The simulation of the rainstorm flood disaster process revealed significant changes in the composition of submerged areas with different degrees of inundation over time.

As shown in Figure 7, during the first 30 min of the model simulation, some areas in Futian District gradually began to produce water with a depth of 0.1 m to 1 m. As the simulation continued for about 90 min, the flooded area with a depth of 0.1 m to 0.5 m gradually stabilized at about 8 km^2, while the flooded area with a water depth of 0.5 m to 1 m gradually stabilized at 3.3 km^2. In addition, with the gradual increase of precipitation intensity, the surface runoff in the areas affected by the rainstorm rapidly formed, and water with a large depth began to appear in Futian District. After 120 min of model simulation, the inundated area with water depth above 1 m continued to increase with the advance of the simulation time.

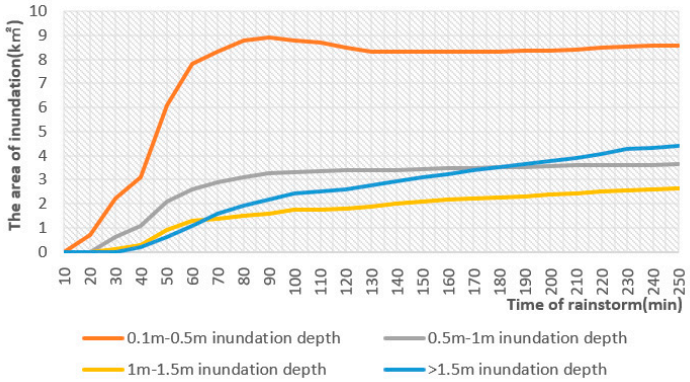

Figure 7. Curves of different inundation areas over time under the once-in-a-century disaster scenario.

3.2. Temporal Changes of Urban Rainstorm Flood Disaster Risk in Building and Road

The changes in urban buildings risk under the three disaster scenarios are shown in Figure 8, among which the average risk of buildings under the morning peak rainfall scenario is the largest, which is 2.1 times the evening peak and 3.2 times the midnight. In the midnight scenario, the population rest in residential buildings late at night, and the risk of buildings shows a dynamic trend of increasing over time, which is obviously consistent with the trend of the change of the degree of inundation of heavy rainfall, and the trend of risk change is only related to the degree of inundation of heavy rainfall. Under the morning peak rainfall scenario, the building risk increases greatly in the early stage of the simulation model, which is caused by the activities of the student population and the working population going to work and others, and then the building risk is temporarily reduced due to the elderly population and random population stopping leisure activities and returning home, and then the risk continues to increase slowly with the degree of inundation of heavy rainfall. This indicates that the changing trend of risk is affected by the evolution process of rainstorm flood disasters and the dynamic activities process of the urban population. Under the evening peak rainfall scenario, the risk of buildings gradually increases with the depth and extent of inundation of rainfall disasters, and then as most of the population agents return home from a day's commuting activities, the average risk of urban buildings decreases slightly due to the low sensitivity of residential buildings and gradually tends to be consistent with the risk trend under midnight rainfall scenario.

In order to explore the influence of crowd activities on the changes of road risk in different rainfall scenarios, the risk of roads is divided into four risk levels based on the natural discontinuity method and concludes the change trends of the number of roads with different risk levels with rainfall time are shown in Figure 9. In the morning peak rainfall scenario, as the total length of road flooding increases and the number of people exposed to the road increases, the number of risky roads gradually increases, reaching a maximum of 520. About two hours after the rainfall, with the end of the morning peak commuting activities, the number of people exposed to the road becomes less and less, and the number of risky roads decreases slightly; In the evening peak rainfall scenario, the number of risky roads reaches a maximum of 603 after around two hours of rainfall and then decreases slightly as the population ends those activities for the day. However,

in the first 4 h of the rainfall scenario, the average number of roads with medium and high risk in the evening peak is about 1.7 times higher than that during the morning peak, which is speculated to be due to the fact that most of the population departs quickly to their destination in the morning peak period, and the population is exposed to the lower duration of the buildings. In the evening peak rainfall scenario, a large number of random population and working populations are still busy with complex social activities, such as shopping malls, park wandering and other travel activities, resulting in a long-term and high level of population exposure to the road, which increases the risk of heavy rainfall and flooding on urban roads in the evening peak rainfall scenario.

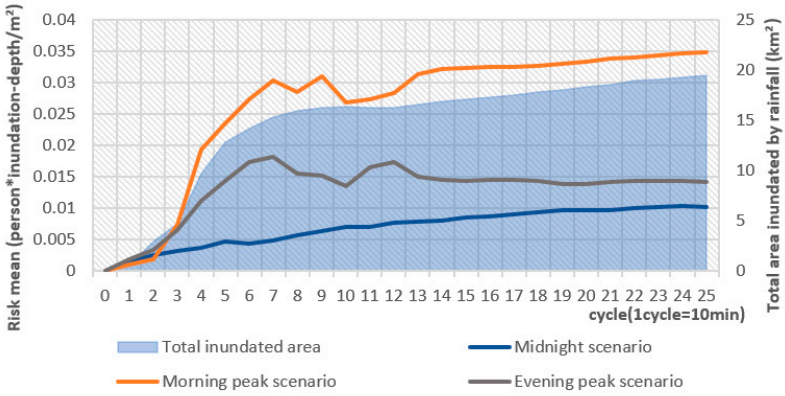

Figure 8. Changes in urban building risks under three rainfall scenarios.

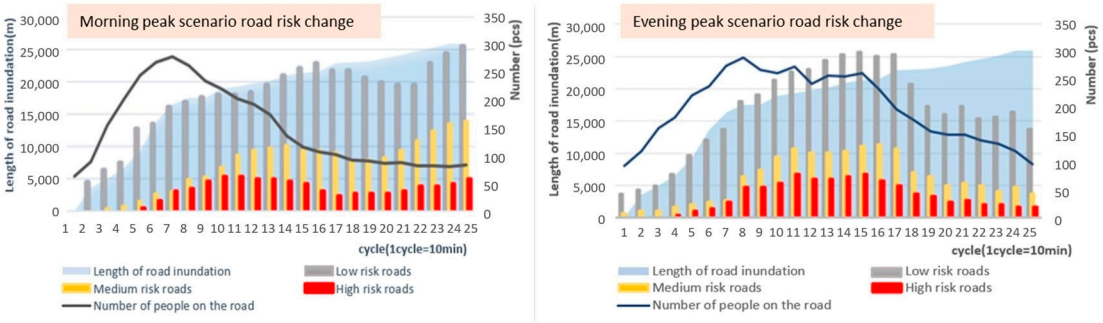

Figure 9. Trends in the number of roads at risk under the morning and evening peak scenarios.

Through a comparative analysis of the risk of urban buildings and roads under the morning and evening peak rainfall scenarios, as shown in Figure 10, it is found that the average roads risk is about three times the average risk of buildings because the disaster sensitivity of the population exposed to the roads is higher than that inside the buildings. In addition, with the expansion of the inundation area of urban rainstorm flood disasters, the risks of buildings and roads are on the rise, but during the morning peak hours, the risks of roads and buildings increase rapidly due to the commuting activities of the crowd and tends to flatten; During the evening peak hours, due to the complex leisure and entertainment activities of the crowd, the roads risk has a continuous upward trend, and the overall buildings risk shows a downward trend, which is caused by the return of the crowd to low-sensitivity residences.

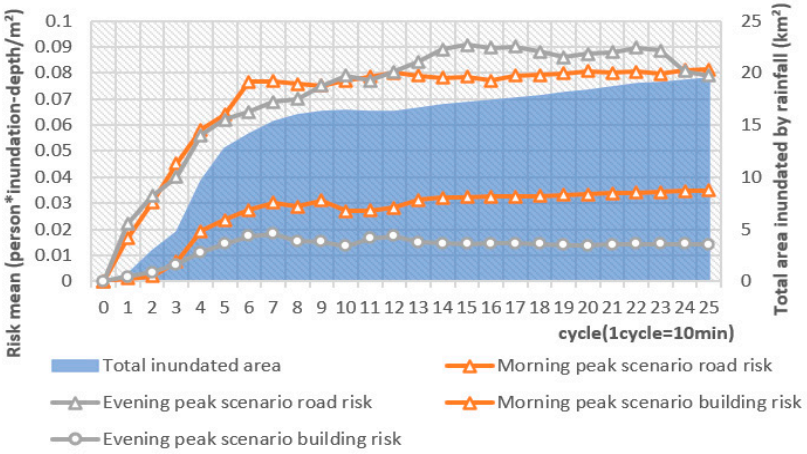

Figure 10. Changes in building and road risk for morning and evening peak rainfall.

3.3. Spatial Changes of Urban Rainstorm Flood Disaster Risk in Building and Road

In order to further explore the influence of crowd activities on the spatial changes of risk of different types of buildings in the city, this study further calculates the proportion of buildings at risk for each type of building in the city and the risk changes trend of each building in the morning disaster scenarios is shown in Figure 11. In the morning peak rainfall scenario, the risk of heavy rainstorm flood is mainly distributed among 251 school buildings and 194 shopping mall buildings. The proportion of risky buildings in schools and shopping malls reaches more than 40%, and the risk of school buildings is the highest, which needs to be attention. The average risk of heavy rainstorm flood for all types of buildings is still the school, followed by industrial buildings and shopping mall buildings, while the average risk and proportion of risk buildings for park and residential buildings are relatively low. This is due to the high flood sensitivity level of school buildings and the large concentration of students, which increases the risk of heavy rainstorm flood, while due to the relatively low population density of parks and residential buildings, the risk and proportion of heavy rainstorm flood are relatively low.

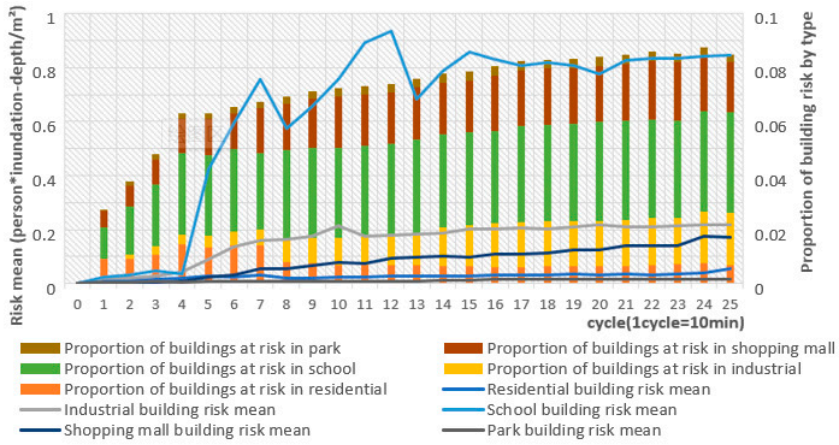

Figure 11. Trends in building type risks under morning peak scenario.

In the evening peak rainfall scenario, the risk trend of each building type in the city is shown in Figure 12. In the first two hours of the model run, school and industrial buildings account for the largest proportion of risk, and then buildings with a high proportion of rainstorm flood disaster risk gradually shifted to shopping malls and finally to residential buildings. This is due to the fact that during the evening peak, as the population leaves work, school, shopping and leisure activities, the urban population gradually shifts to shopping malls, parks or residential buildings. In the evening peak rainfall scenario, the

average risk of rainstorm flood for all types of buildings is still the highest in schools, shopping malls and industrial areas, and then the proportion of risks in schools, shopping malls and other buildings show a downward trend due to the return of to their residences.

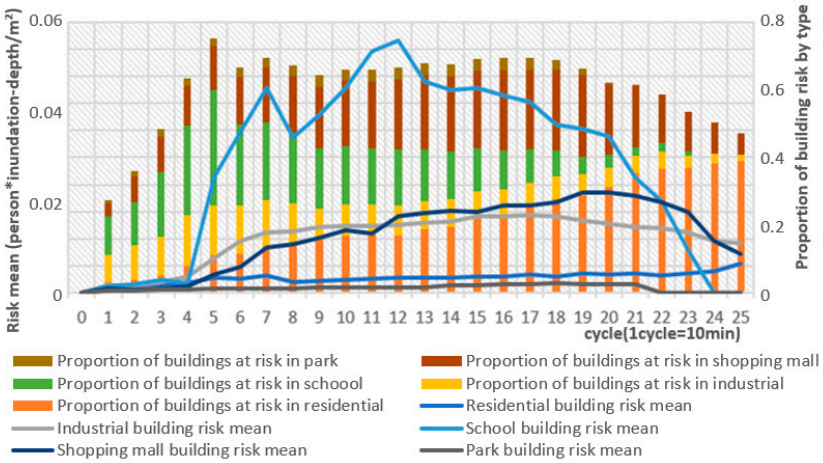

Figure 12. Trends in building types risk under evening peak scenario.

In order to further explore the distribution of high-risk roads of rainstorm flood disasters under crowd activities in the study area, this study counts the risky roads with high-risk levels in the morning and evening peak disaster scenarios, as shown in Table 4. It can be seen that due to the high sensitivity level of roads, such as Xiangxuan Road, Meiting Road, and Bagua Road, the risk level and the risk duration in the risk state are much higher than those of main roads and secondary roads.

Table 4. High-risk sections of urban storm flooding.

Road Name	Type	Risk Level	Average Risk Time (min)
Xiangxuan Road	community branch roads	High	115
Xianggang West Road	secondary road	High	95
Meikang Road	community branch roads	High	115
Meiting Road	community branch roads	High	100
Mintian Road	community branch roads	High	90
Xinzhou Road	motorcycle roads	High	105
Fuchai Road	community branch roads	High	100
Bagua Road	motorcycle roads	High	115

In order to further compare the spatial changes of urban rainstorm flood risk after 1 h, 2 h, and 3 h of model runs in the three rainfall scenarios, this study divides the buildings risk, and road risk into four risk levels based on the natural discontinuity method, and the results are shown in Figure 13. The figure indicates that the risk range of urban rainstorm floods with daytime rainfall is much larger than that of midnight rainfall. In the subfigure labeled "Midnight scenario simulation 3 h", the risk of urban rainstorm flood in the midnight rainfall scenario is only distributed in residential buildings, while the spatial impact of urban rainstorm flood risk in the morning peak rainfall scenario is the largest, as shown in the sub-figure labeled "Morning peak scenario simulation 3 h". This is because the urban population activities are wide during the day, and the sensitivity of industrial, schools and shopping malls buildings to the risk of heavy rainfall is much higher than that of residential buildings, so the average risk and risk range of buildings with daytime rainfall being much greater than that of nighttime rainfall.

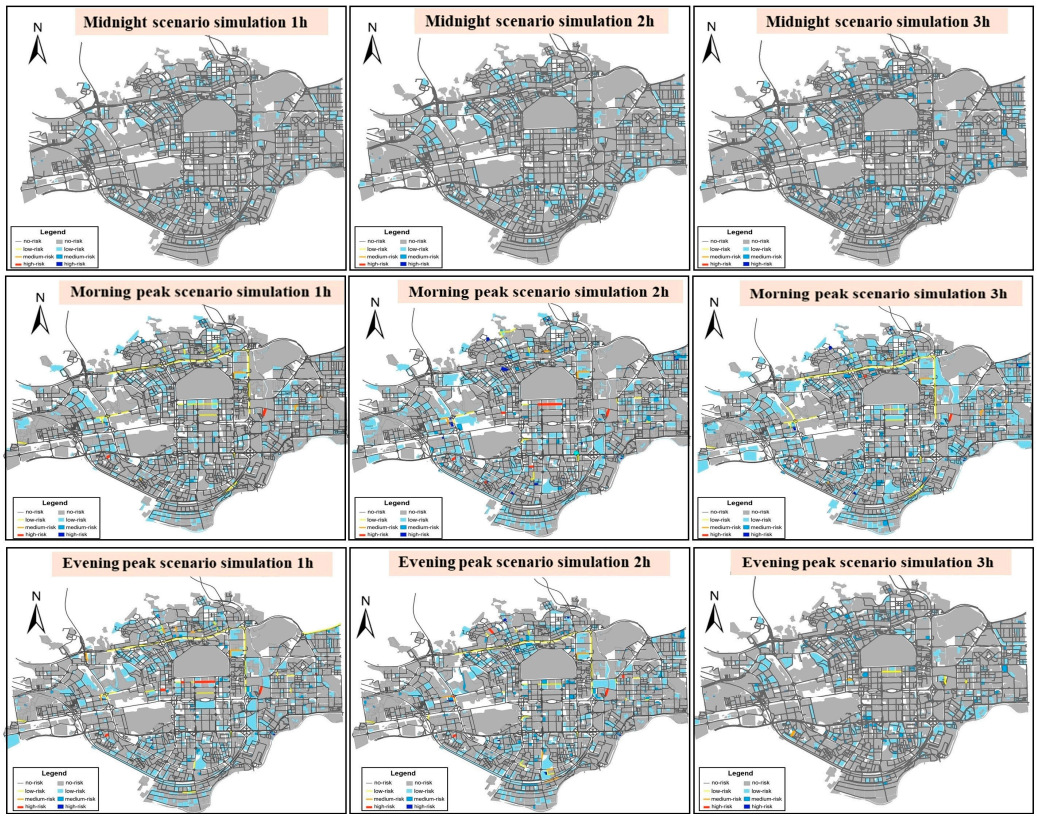

Figure 13. Spatial evolution of urban rainstorm flood disaster risk in three rainfall scenarios.

As depicted in the subfigure labeled "Evening peak scenario simulation 3 h", it is found that the spatial distribution of risk after 3 h simulation is slightly different from that after 3 h simulation in the midnight scenario, but it is very similar. This is because most people have finished their evening peak commute and returned to their homes at this time, and the spatial distribution of the population gradually approaches that of the midnight scenario. In addition, the risk of urban rainstorm flood is related to the spatial distribution of the urban population; in the morning and evening peak rainfall scenario, the risk of urban rainstorm flood shows an opposite spatial transfer trend with crowd activities. In the morning peak period, the risk of urban heavy rainstorm flood shifts from residential buildings to industrial buildings, schools, shopping malls and other buildings. Conversely, in the evening peak period, the risk shifts in the opposite direction compared to the morning peak rainfall scenario, gradually shifting to residential buildings due to crowd activities.

4. Discussion

From the perspective of complex systems, flood disaster risks are a product of the coupling of natural processes and social activities. In this study, besides the urban flooding process, crowd activities are included in the rainstorm flood disaster risk assessment. A risk simulation model of urban rainstorm flood disasters based on ABM considering the crowds' daily activities is constructed. It is found that rainstorm flooding remains the primary factor influencing the risk of flood disasters, but crowd activities greatly amplify this risk and impact its spatial distribution. For instance, during midnight, the risk is more affected by surface inundation and is mainly concentrated in urban residential areas. However, during morning and evening peaks, increased crowd activities pose a greater risk on roads due to commuting, and there is a shift from residential areas to industrial areas, schools, shopping malls, etc., during the morning peak and the reverse during the evening peak. Compared with the previous risk assessment based on the dynamic

rainstorm flood disasters process, it can further reflect the impact of urban rainstorm flood disasters brought by crowd activities. This can lead to a more comprehensive and accurate assessment of urban rainstorm flood disaster risks and further reveal the mechanisms of the impact of human activities on the changes of disaster risks, which can then be used to provide detailed emergency prevention suggestions for urban crowd activity warnings and rainstorm flood disaster management.

In this study, three scenarios (midnight, morning peak, and evening peak) are set up to explore the effect of crowd activity patterns on rainstorm flood disaster risk. It is found that the risk of a rainstorm flood disaster is greatly different when it occurs in different periods, influenced by the activity patterns in different periods. The average risk of urban buildings and roads during morning and evening peak hours is much higher than during midnight hours. Especially during the crowded morning and evening peak hours, the risk of school and shopping mall buildings is significantly higher compared to other building types. Additionally, the spatial distribution of risks is wider and more dispersed during morning and evening peak hours. This is because the spatial migration activities of the urban crowd during the morning peak and evening peak are frequent and complex, and the spatial exposure of the urban population as the direct object of the disaster will directly affect the size and spatial distribution of disaster risk. The findings of this study revealed how crowd activities affect the dynamic change of rainstorm flood disaster risk from two dimensions of time and space, which provides a new research perspective for the dynamic risk assessment of rainstorm flood disasters based on disaster consequences. It also provides theoretical support for government departments to set up a refined contingency plan for rainstorm flood disasters according to the disaster consequences.

Although direct validation of the results of urban rainstorm flood disaster risk is challenging due to the complexity and unpredictability of real-world events, the study recognizes the importance of validating the constructed model to demonstrate its reliability. For the urban rainstorm flood modelling simulation model, the parameters are calibrated using real rainfall inundation data on 29 August 2018 and 11 April 2019 in Shenzhen. The simulated results are validated by comparing them with monitoring data from waterlogging points. The population numbers for each type are determined using data from the Shenzhen Statistical Yearbook, ensuring that our model accurately represents the real demographic composition. Additionally, crowd activity rules are established based on actual traffic investigations in Shenzhen and literature summarizing the temporal and spatial activity patterns of the urban population. These rules align with actual urban population activities and significantly reflect the travel status of the urban population in the study area on a typical day, providing a sound basis for the behavior rules of the agents in our model. Furthermore, the population on the road during morning peak and evening peak are in accordance with the actual observed situation, suggesting that our model can realistically reflect the patterns of urban crowd activities during different time periods. After running the urban rainstorm flood disaster risk simulation model several times, we observed that the results have almost no deviation and are consistent with actual life experiences. This reproducibility indicates that our model can reliably capture the dynamics of rainstorm flood risk in urban areas. While direct validation of complex models like ours is challenging, we believe that these validation aspects provide reasonable evidence of the credibility and robustness of our constructed model.

5. Conclusions

Frequent human activities increase the risk of urban flood disasters. From the perspective of natural–social coupled systems, this research proposes a risk simulation model of urban rainstorm flood disaster, which combines agent-based modeling (ABM) of daily crowd activities with the SWMM-LISFLOOD urban flooding simulation mode in order to detect the temporal and spatial changes of the rainstorm flood disaster risk of buildings and roads. Additionally, three scenarios, midnight, morning peak and evening peak, are

designed to explore the effects of different crowd activities models on flood disaster risk in once-in-a-century rainstorms. The conclusions are as follows:

(1) The risk of rainstorm flood disasters is influenced by both the urban flooding process and the activities of urban crowds. As urban inundation increases, the risk also increases. However, crowd activities can amplify this risk. During the morning peak hours, the risk for roads and buildings increases rapidly due to commuting activities and then stabilizes. During the evening peak hours, there is a sustained and long-lasting upward trend in road risks due to leisure and entertainment activities.

(2) The risk of rainstorm flood disasters for buildings and roads varies significantly over time. The average risk for buildings is highest during the morning peak hours, more than twice the average risk during the evening peak hours. The average risk for roads is basically the same during morning and evening peak hours, but the number of roads at risk is higher during the evening peak hours. Buildings and roads are at the lowest risk during midnight rainfall scenarios. Roads have a higher average risk than buildings during morning and evening peak hours.

(3) The spatial distribution of flood risk shifts with the social activities of urban crowds. During the morning peak hours, the risk shifts from residential buildings to industrial buildings, schools, shopping malls, and other areas. As crowds end their daily activities during the evening peak hours, the risk gradually shifts back to residential buildings.

Based on the research findings, it is recommended that the government should improve and integrate early warning systems that consider both natural factors, such as rainfall intensity, and human factors, such as crowd activities. Providing timely and accurate flood warnings to the public and relevant authorities will facilitate proactive responses. Moreover, the government should develop comprehensive emergency response plans for different risk zones that account for various rainstorm flood disaster scenarios, including morning and evening peak hours.

While the research contributes valuable insights into the risk simulation of urban rainstorm flood disasters, the need for further advancements in modeling crowd activities and exploring their intricate connections with disaster dynamics is evident. The simulation of urban crowd activities only considers the age of the population. However, in future research, big data will be used to describe the spatiotemporal activity patterns of urban crowd activities in a more refined manner. By improving the parameters related to the individual characteristics of the population in the simulation model, deeper insights into the change process of rainstorm flood disaster risk under the influence of urban crowd activities can be gained. Additionally, the complex interaction relationship between rainstorm flood disasters and crowd activities has not been fully explored. For instance, the activity patterns of the urban crowd may change after receiving rainstorm information or during a disaster event. To address this limitation, future studies will focus on investigating specific disaster situations and early warning measures, allowing for a more comprehensive understanding of the dynamic interactions between rainstorm flood disasters and crowd activities.

Author Contributions: Conceptualization, J.H. and T.P.; Methodology, J.H., Z.L. and Z.W.; Software, T.P., Z.L. and Z.W.; Validation, H.W.; Formal analysis, J.H.; Data curation, Z.L. and Z.W.; Writing—original draft, T.P.; Writing—review and editing, J.H.; Supervision, J.H.; Project administration, H.W.; Funding acquisition, H.W. All authors have read and agreed to the published version of the manuscript.

Funding: This research was funded by he National Natural Science Foundation of China [Grant No.42171081 and No.91846203].

Data Availability Statement: Road network, population data, and rainstorm flood inundation are openly available; building, drainage network, and waterlogging points monitoring data are available from Shenzhen Hydrology Bureau. Restrictions apply to the availability of these data, which were used under license for this study. Data are available with the permission of the Shenzhen Hydrology Bureau.

Conflicts of Interest: The authors declare no conflict of interest.

References

1. Li, Y.; Ye, S.; Wu, Q.; Wu, Y.; Qian, S. Analysis and countermeasures of the "7.20" Flood in Zhengzhou. *J. Asian Archit. Build. Eng.* **2023**, 1–17. [CrossRef]
2. Foudi, S.; Osés-Eraso, N.; Tamayo, I. Integrated spatial flood risk assessment: The case of Zaragoza. *Land Use Policy* **2015**, *42*, 278–292. [CrossRef]
3. Ma, B. Definition and expression methods for natural disaster risk. *J. Catastrophol.* **2015**, *30*, 016–020.
4. Zheng, Q.; Shen, S.-L.; Zhou, A.; Lyu, H.-M. Inundation risk assessment based on G-DEMATEL-AHP and its application to Zhengzhou flooding disaster. *Sustain. Cities Soc.* **2022**, *86*, 104138. [CrossRef]
5. Pelling, M.; Maskrey, A.; Ruiz, P.; Hall, L.; Peduzzi, P.; Dao, Q.-H.; Mouton, F.; Herold, C.; Kluser, S. Reducing disaster risk: A challenge for development. In *United Nations Development Bank, Bureau for Crisis Prevention and Recovery, New York*; WHO: Geneva, Switzerland, 2004. Available online: https://www.undp.org/publications/reducing-disaster-risk-challenge-development (accessed on 25 July 2023).
6. Koks, E.E.; Jongman, B.; Husby, T.G.; Botzen, W.J. Combining hazard, exposure and social vulnerability to provide lessons for flood risk management. *Environ. Sci. Policy* **2015**, *47*, 42–52. [CrossRef]
7. Li, C.; Tian, J.; Shen, R. Review on assessment of flood and waterlogging risk. *J. Catastrophology* **2020**, *35*, 131–136.
8. Li, C.; Cheng, X.; Li, N.; Du, X.; Yu, Q.; Kan, G. A framework for flood risk analysis and benefit assessment of flood control measures in urban areas. *Int. J. Environ. Res. Public Health* **2016**, *13*, 787. [CrossRef]
9. Lyu, H.-M.; Sun, W.-J.; Shen, S.-L.; Arulrajah, A. Flood risk assessment in metro systems of mega-cities using a GIS-based modeling approach. *Sci. Total Environ.* **2018**, *626*, 1012–1025. [CrossRef]
10. Zhang, J.; Chen, Y. Risk assessment of flood disaster induced by typhoon rainstorms in Guangdong province, China. *Sustainability* **2019**, *11*, 2738. [CrossRef]
11. Falter, D.; Dung, N.; Vorogushyn, S.; Schröter, K.; Hundecha, Y.; Kreibich, H.; Apel, H.; Theisselmann, F.; Merz, B. Continuous, large-scale simulation model for flood risk assessments: Proof-of-concept. *J. Flood Risk Manag.* **2016**, *9*, 3–21. [CrossRef]
12. Tanaka, T.; Kiyohara, K.; Tachikawa, Y. Comparison of fluvial and pluvial flood risk curves in urban cities derived from a large ensemble climate simulation dataset: A case study in Nagoya, Japan. *J. Hydrol.* **2020**, *584*, 124706. [CrossRef]
13. Li, G.; Zhao, H.; Liu, C.; Wang, J.; Yang, F. City Flood Disaster Scenario Simulation Based on 1D–2D Coupled Rain–Flood Model. *Water* **2022**, *14*, 3548. [CrossRef]
14. Rubinato, M.; Nichols, A.; Peng, Y.; Zhang, J.-m.; Lashford, C.; Cai, Y.-p.; Lin, P.-z.; Tait, S. Urban and river flooding: Comparison of flood risk management approaches in the UK and China and an assessment of future knowledge needs. *Water Sci. Eng.* **2019**, *12*, 274–283. [CrossRef]
15. Yan, X.; Xu, K.; Feng, W.; Chen, J. A rapid prediction model of urban flood inundation in a high-risk area coupling machine learning and numerical simulation approaches. *Int. J. Disaster Risk Sci.* **2021**, *12*, 903–918. [CrossRef]
16. Yin, Z.e.; Yin, J.; Xu, S.; Wen, J. Community-based scenario modelling and disaster risk assessment of urban rainstorm waterlogging. *J. Geogr. Sci.* **2011**, *21*, 274–284. [CrossRef]
17. Doocy, S.; Daniels, A.; Murray, S.; Kirsch, T.D. The human impact of floods: A historical review of events 1980–2009 and systematic literature review. *PLoS Curr.* **2013**, *5*. Available online: https://www.ncbi.nlm.nih.gov/pmc/articles/PMC3644291/ (accessed on 25 July 2023). [CrossRef] [PubMed]
18. Rehman, J.; Sohaib, O.; Asif, M.; Pradhan, B. Applying systems thinking to flood disaster management for a sustainable development. *Int. J. Disaster Risk Reduct.* **2019**, *36*, 101101. [CrossRef]
19. Collins, A.E. Advancing the disaster and development paradigm. *Int. J. Disaster Risk Sci.* **2018**, *9*, 486–495. [CrossRef]
20. Hallegatte, S.; Vogt-Schilb, A.; Rozenberg, J.; Bangalore, M.; Beaudet, C. From poverty to disaster and back: A review of the literature. *Econ. Disasters Clim. Change* **2020**, *4*, 223–247. [CrossRef]
21. Abebe, Y.A.; Ghorbani, A.; Nikolic, I.; Vojinovic, Z.; Sanchez, A. A coupled flood-agent-institution modelling (CLAIM) framework for urban flood risk management. *Environ. Model. Softw.* **2019**, *111*, 483–492. [CrossRef]
22. O'Connell, P.; O'Donnell, G. Towards modelling flood protection investment as a coupled human and natural system. *Hydrol. Earth Syst. Sci.* **2014**, *18*, 155–171. [CrossRef]
23. Zhuo, L.; Han, D. Agent-based modelling and flood risk management: A compendious literature review. *J. Hydrol.* **2020**, *591*, 125600. [CrossRef]
24. Lai, W.; Li, W.; Wang, H.; Huang, Y.; Wu, X.; Sun, B. Dynamic building risk assessment theoretic model for rainstorm-flood utilization ABM and ABS. In *MIPPR 2015: Remote Sensing Image Processing, Geographic Information Systems, and Other Applications*; SPIE: Bellingham, WA, USA, 2015; pp. 214–220.
25. Dawson, R.J.; Peppe, R.; Wang, M. An agent-based model for risk-based flood incident management. *Nat. Hazards* **2011**, *59*, 167–189. [CrossRef]
26. Li, W.; Guo, X.; Mao, X.; Xiao, D.; Lai, W.; Wang, H. The dynamic population risk assessment model for rainstorm-flood utilization multi-agent. *J. Catastrophology* **2015**, *30*, 80–87.
27. Dai, Q.; Zhu, X.; Zhuo, L.; Han, D.; Liu, Z.; Zhang, S. A hazard-human coupled model (HazardCM) to assess city dynamic exposure to rainfall-triggered natural hazards. *Environ. Model. Softw.* **2020**, *127*, 104684. [CrossRef]
28. Turner, J.R.; Baker, R.M. Complexity theory: An overview with potential applications for the social sciences. *Systems* **2019**, *7*, 4. [CrossRef]

29. Yao, Y.; Liu, X.; Li, X.; Zhang, J.; Liang, Z.; Mai, K.; Zhang, Y. Mapping fine-scale population distributions at the building level by integrating multisource geospatial big data. *Int. J. Geogr. Inf. Sci.* **2017**, *31*, 1220–1244. [CrossRef]
30. Terti, G.; Ruin, I.; Anquetin, S.; Gourley, J.J. Dynamic Vulnerability Factors for Impact-Based Flash Flood Prediction. *Nat. Hazards* **2015**, *79*, 1481–1497. [CrossRef]
31. Wu, X.; Wang, Z.; Guo, S.; Liao, W.; Zeng, Z.; Chen, X. Scenario-based projections of future urban inundation within a coupled hydrodynamic model framework: A case study in Dongguan City, China. *J. Hydrol.* **2017**, *547*, 428–442. [CrossRef]
32. Neal, J.C.; Bates, P.D.; Fewtrell, T.J.; Hunter, N.M.; Wilson, M.D.; Horritt, M.S. Distributed whole city water level measurements from the Carlisle 2005 urban flood event and comparison with hydraulic model simulations. *J. Hydrol.* **2009**, *368*, 42–55. [CrossRef]
33. Gong, P.; Chen, B.; Li, X.; Liu, H.; Wang, J.; Bai, Y.; Chen, J.; Chen, X.; Fang, L.; Feng, S. Mapping essential urban land use categories in China (EULUC-China): Preliminary results for 2018. *Sci. Bull.* **2020**, *65*, 182–187. [CrossRef]
34. Xu, Y.; Shaw, S.-L.; Zhao, Z.; Yin, L.; Fang, Z.; Li, Q. Understanding aggregate human mobility patterns using passive mobile phone location data: A home-based approach. *Transportation* **2015**, *42*, 625–646. [CrossRef]
35. Zhu, X.; Dai, Q.; Han, D.; Zhuo, L.; Zhu, S.; Zhang, S. Modeling the high-resolution dynamic exposure to flooding in a city region. *Hydrol. Earth Syst. Sci.* **2019**, *23*, 3353–3372. [CrossRef]
36. Tang, L.; Gao, J.; Ren, C.; Zhang, X.; Yang, X.; Kan, Z. Detecting and evaluating urban clusters with spatiotemporal big data. *Sensors* **2019**, *19*, 461. [CrossRef]
37. Barbosa, H.; Barthelemy, M.; Ghoshal, G.; James, C.R.; Lenormand, M.; Louail, T.; Menezes, R.; Ramasco, J.J.; Simini, F.; Tomasini, M. Human Mobility: Models and Applications. *Phys. Rep.* **2018**, *734*, 1–74. [CrossRef]
38. Demissie, M.G.; Phithakkitnukoon, S.; Kattan, L.; Farhan, A. Understanding Human Mobility Patterns in a Developing Country Using Mobile Phone Data. *Data Sci. J.* **2019**, *18*, 1. [CrossRef]
39. Dong, P.; Ramesh, S.; Nepali, A. Evaluation of small-area population estimation using LiDAR, Landsat TM and parcel data. *Int. J. Remote Sens.* **2010**, *31*, 5571–5586. [CrossRef]